



TITLE:

# Unmanned aerial vehicles and deep learning for assessment of anthropogenic marine debris on beaches on an island in a semi-enclosed sea in Japan

AUTHOR(S):

Takaya, Kosuke; Shibata, Atsuki; Mizuno, Yuji; Ise, Takeshi

---

CITATION:

Takaya, Kosuke ...[et al]. Unmanned aerial vehicles and deep learning for assessment of anthropogenic marine debris on beaches on an island in a semi-enclosed sea in Japan. *Environmental Research Communications* 2022, 4(1): 015003.

ISSUE DATE:

2022-01

URL:

<http://hdl.handle.net/2433/276950>

RIGHT:

© 2022 The Author(s). Published by IOP Publishing Ltd; Original content from this work may be used under the terms of the Creative Commons Attribution 4.0 licence. Any further distribution of this work must maintain attribution to the author(s) and the title of the work, journal citation and DOI.

# ENVIRONMENTAL RESEARCH COMMUNICATIONS

---

PAPER • OPEN ACCESS

## Unmanned aerial vehicles and deep learning for assessment of anthropogenic marine debris on beaches on an island in a semi-enclosed sea in Japan

To cite this article: Kosuke Takaya *et al* 2022 *Environ. Res. Commun.* **4** 015003

View the [article online](#) for updates and enhancements.

You may also like

- [Coastal margins and backshores represent a major sink for marine debris: insights from a continental-scale analysis](#)  
Arianna Olivelli, Britta Denise Hardesty and Chris Wilcox
- [Analysis of sources and composition of marine debris in western and southern Aceh, Indonesia](#)  
R Fitria, F Diana, E Riani et al.
- [Marine debris monitoring in the coastal area of the District of Banyuwangi, Indonesia: Characterization of the debris type and composition](#)  
E. Nurhayati, B.V. Tangahu, I.R. Mahardini et al.

## Environmental Research Communications



### PAPER

# Unmanned aerial vehicles and deep learning for assessment of anthropogenic marine debris on beaches on an island in a semi-enclosed sea in Japan

#### OPEN ACCESS

RECEIVED  
10 October 2021

REVISED  
4 December 2021

ACCEPTED FOR PUBLICATION  
30 December 2021

PUBLISHED  
17 January 2022

Original content from this work may be used under the terms of the [Creative Commons Attribution 4.0 licence](#).

Any further distribution of this work must maintain attribution to the author(s) and the title of the work, journal citation and DOI.



Kosuke Takaya<sup>1</sup> , Atsuki Shibata<sup>2,3</sup>, Yuji Mizuno<sup>4</sup> and Takeshi Ise<sup>5</sup>

<sup>1</sup> Graduate School of Agriculture, Kyoto University, Oiwake, Kitashirakawa Sakyo-ku, Kyoto 606-8502, Japan

<sup>2</sup> Center for the Promotion of Interdisciplinary Education and Research, Kyoto University, Oiwake, Kitashirakawa Sakyo-ku, Kyoto 606-8502, Japan

<sup>3</sup> Department of Geography, Faculty of Letters, Nara University, 1500 Misasagi-cho, Nara-shi, Nara 631-8502, Japan

<sup>4</sup> YM Lab., 702 Minamisemba SOHO biru, 4-10-5 Minamisemba, Chuo-ku, Osaka 542-0081, Japan

<sup>5</sup> Field Science Education and Research Center, Kyoto University, Oiwake, Kitashirakawa Sakyo-ku, Kyoto 606-8502, Japan

E-mail: [takaya.kosuke.25a@st.kyoto-u.ac.jp](mailto:takaya.kosuke.25a@st.kyoto-u.ac.jp)

**Keywords:** anthropogenic marine debris, unmanned aerial vehicles, deep learning, beach census method

Supplementary material for this article is available [online](#)

### Abstract

The increasing prevalence of marine debris is a global problem, and urgent action for amelioration is needed. Identifying hotspots where marine debris accumulates will enable effective control; however, knowledge on the location of accumulation hotspots remains incomplete. In particular, marine debris accumulation on beaches is a concern. Surveys of beaches require intensive human effort, and survey methods are not standardized. If marine debris monitoring is conducted using a standardized method, data from different regions can be compared. With an unmanned aerial vehicle (UAV) and deep learning computational methods, monitoring a wide area at a low cost in a standardized way may be possible. In this study, we aimed to identify marine debris on beaches through deep learning using high-resolution UAV images by conducting a survey on Narugashima Island in the Seto Inland Sea of Japan. The flight altitude relative to the ground was set to 5 m, and images of a 0.81-ha area were obtained. Flight was conducted twice: before and after the beach cleaning. The combination of UAVs equipped with a zoom lens and operation at a low altitude allows for the acquisition of high resolution images of 1.1 mm/pixel. The training dataset (2970 images) was annotated by using VoTT, categorizing them into two classes: ‘anthropogenic marine debris’ and ‘natural objects.’ Using RetinaNet, marine debris was identified with an average sensitivity of 51% and a precision of 76%. In addition, the abundance and area of marine debris coverage were estimated. In this study, it was revealed that the combination of UAVs and deep learning enables the effective identification of marine debris. The effects of cleanup activities by citizens were able to be quantified. This method can widely be used to evaluate the effectiveness of citizen efforts toward beach cleaning and low-cost long-term monitoring.

### Introduction

The rapid increase in anthropogenic marine debris has been recognized as a global environmental problem (Ostle *et al* 2019). The majority of marine debris consists of plastic (Barnes *et al* 2009), and it is estimated that 4.4–12.7 million metric tons of plastic are discharged into the ocean annually (Jambeck *et al* 2015). Previous studies have indicated that in the western Pacific Ocean, particularly in the Kuroshio Current area, more than 3.5 million pieces of debris per square kilometer at the ocean surface may be present (Yamashita and Tanimura 2007). The problem with marine debris is not only the amount of inflow but also its persistence. Plastics are chemically resistant to degradation and remain in the marine environment for hundreds to

thousands of years (Derraik 2002). Therefore, they continue to accumulate over a long time and have a variety of effects, such as an impact on tourism due to aesthetic degradation and ingestion by marine organisms. In addition, plastic fragmentation and degradation driven by environmental factors such as ultraviolet (UV) light result in small particles that are known as microplastics (Andrady 2011, Cole *et al* 2011).

Marine debris affects the human economy, particularly, shipping, fishing, and tourism (McIlgorm *et al* 2011). For example, in tourist destinations, aesthetic degradation by marine litter decreases revenue from tourism, and local authorities need to bear the cost of cleanup (Iñiguez *et al* 2016). The dynamics of marine debris widely vary, and heavier items may accumulate on the seafloor. There have been attempts to collect marine debris, but these are costly and sometimes dangerous. For instance, in a project to remove debris from the seabed in South Korea, about 460 tons of trash were recovered at a cost of \$3.8 million, and fatal incidents were involved (Cho 2011).

Marine ecosystems are also affected by marine debris. Ingestion and entanglement are two impacts of marine debris on marine organisms (Derraik 2002). Marine organisms from a wide range of taxonomic groups ingest marine debris, sometimes leading to death (Gregory 2009). Entanglement in discarded fishing gear-related debris is known as ‘ghost fishing’ and is recognized as a serious threat. At least 690 species are threatened by marine debris, of which at least 17% are classified as near-threatened or higher on the IUCN Red List (Gall and Thompson 2015). To mitigate the impact of marine debris, a quantitative assessment of the distribution of marine debris is the first step. Once the location and amount of marine debris present are understood, the removal of marine debris can be implemented.

The accumulation of marine debris has been confirmed over a wide area from the Arctic to the Antarctic and in the deep sea (Woodall *et al* 2014). However, the amount of plastic debris observed in the ocean is much lower than that previously expected (Cózar *et al* 2014). Various studies have been conducted to determine where the ‘missing plastic’ exists (Law and Thompson 2014). This ‘missing plastic’ may be drifting in currents (Eriksen *et al* 2014) or water columns (Dai *et al* 2018) or is accumulating on the seafloor (Chiba *et al* 2018). However, the importance of focusing on beaches has been highlighted (Brennan *et al* 2018, Olivelli *et al* 2020). About half of the world’s population lives near the coast, making coastal areas hotspots for microplastic pollution (Cole *et al* 2011). Shorelines are also strongly influenced by terrestrial factors such as stormwater and road distribution (Willis *et al* 2017), and backshore areas with vegetation can be a sink for large marine debris (Olivelli *et al* 2020). In addition, plastic products on beaches are exposed to UV light that causes photo-oxidative degradation (Singh and Sharma 2008 Sathish *et al* 2019). On beaches in the daylight, the thermal degradation of plastic progress faster than in seawater (Andrady 2011).

In recent years, unmanned aerial vehicles (UAVs) have been used in a wide range of research fields (Jiménez López and Mulero-Pázmány 2019). They are also used to survey marine debris on beaches (Kako *et al* 2012, Bao *et al* 2018, Deidun *et al* 2018, Andriolo *et al* 2020, Gonçalves *et al* 2020, Lo *et al* 2020, Merlini *et al* 2020). UAVs have the advantage of cost effectiveness and the ability to obtain high-resolution images. Studies have conducted marine debris surveys using satellite images, but the high cost and low resolution of the data have been issues. For example, WorldView-4 satellite imagery, with a resolution of about 0.3 m, cannot detect the majority of marine debris on beaches (Topouzelis *et al* 2019). UAVs also facilitate surveys in difficult to access areas such as islands (Lavers and Bond 2017). In addition, UAVs can be used to collect substantial data using a standardized method and compare the distribution of marine debris from different locations. However, the analysis of image data taken by UAVs remains labor-intensive (Jiménez López and Mulero-Pázmány 2019). Deep learning can improve the efficiency of data processing and analysis. However, research on the automatic identification of marine debris from UAV images is a new field, and there are few previous studies on this topic (Martin *et al* 2018, Fallati *et al* 2019, Kako *et al* 2020, Martin *et al* 2021, Papakonstantinou *et al* 2021).

In this study, we aimed to identify anthropogenic marine debris on a beach via high-resolution UAV images using deep learning. The challenges we hope to address in this study are (1) whether UAV images are suitable for automatic identification by deep learning and (2) whether identifying anthropogenic marine debris from the variety of objects present on the beach is possible. If these can be accomplished, it will be possible to survey a wide area with a standardized protocol, which could significantly improve the world’s future marine debris management.

## Methods

### Study area

The Seto Inland Sea is the largest semi-enclosed sea in Japan, with about 31 million residents, more than 700 islands, and a total coastline of about 7,230 km. The climate is mild throughout the year, and the landscape attracts many tourists. The estimated total annual inflow of marine debris into the Seto Inland Sea is 4,500 tons, of which about 70% comes from land (Fujieda *et al* 2010). Training and test images were taken at a site located on

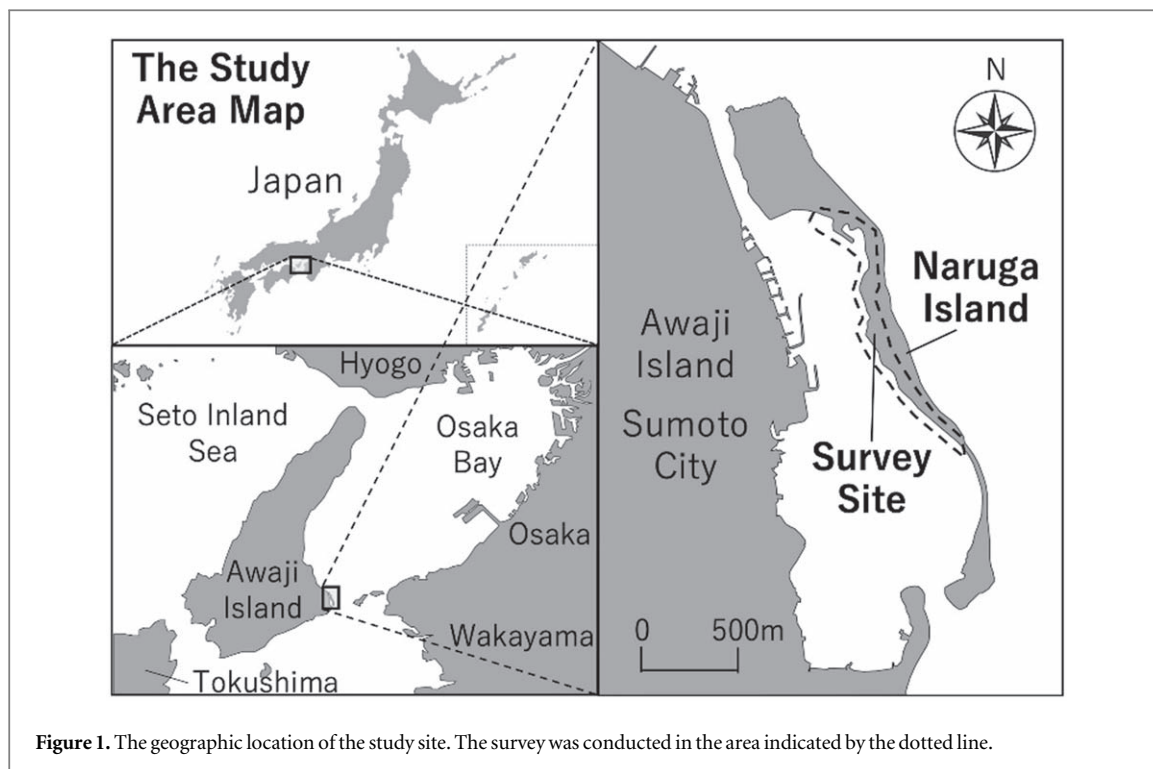


**Figure 1.** The geographic location of the study site. The survey was conducted in the area indicated by the dotted line.

Narugashima Island (34.288351N, 134.952303E) in Hyogo Prefecture (figure 1). Narugashima Island is located in the southeastern part of Awajishima Island. The island has an area of about 25-ha and a total length of about 3 km. There are beaches on the east and west sides, facing Osaka Bay and Yura Bay, respectively. The shorelines of this island are strongly affected by tides, waves, and winds, and a large quantity of marine debris is therefore accumulated. This area belongs to Setonaikai National Park, so local volunteers engage in cleanup activities once a year. Preliminary investigations showed many plastic products drifting on the west rather than the east side of the island (figure 2). Both beaches were set as UAV photography areas to collect the training images.

### UAV survey protocols

The DJI Mavic 2 zoom was used in this study. This UAV is equipped with a 24–48 mm optical zoom lens and a camera with a 1/2.3 CMOS and a 12.4 M pixel sensor. The field of view (FOV) is 83° for the 24-mm zoom and 48° for the 48-mm zoom. It is possible to obtain higher-resolution images with the zoom lens. The flight route was mapped using the DJI GS Pro application, which allows the user to set the flight area and speed in advance and check the shooting status in real time. A 0.81-ha flight plan was created in advance, and shooting was conducted on November 27 and December 4, 2020, and January 25, 2021. Since the flight time of one battery is only 26 min, the battery was continuously replaced. The operators walked on the beach alongside the UAV and used a Jackery portable battery 700 to recharge the depleted batteries for reuse. The flight altitude was set to 5 m, calculated at the point where the UAV took off; therefore, the exact altitude may slightly vary for each image. The shooting interval was set for 50% horizontal and 50% vertical image overlap. The camera's ISO, aperture, and shutter speed were set to AUTO mode, and images with a resolution of 4000 × 3000 pixels were recorded. In this study, the images obtained from the survey of Narugashima Island on November 27, 2020, were used as the training images (table 1). In addition, to improve the model, training images that contained only a PET bottle were obtained from the Kamigamo test site of the Kyoto University Field Science Center on December 16, 2020. Since the cleanup activity was performed on this island on December 5, test images were acquired before and after the day to evaluate the effectiveness of the cleanup activity. Finally, 4,421 test images from the west beach were obtained from Narugashima Island's survey on December 4, 2020, and January 25, 2021.

### The deep learning algorithm

#### Annotations

We annotated images using VoTT, an open-source labeling software developed by Microsoft. We annotated a total of 2,970 images by classifying them into either 'anthropogenic marine debris' or 'natural objects' that mainly consisted of large driftwood. Marine debris larger than 100 pixels was annotated. The classified images were exported in Pascal VOC format and used for training. In this study, 80% of the images were set as training data and 20% were used as validation data.



**Figure 2.** Anthropogenic marine debris observed at the study site. (A) On the west beach taken from the UAV; (B) Taken from the UAV at an altitude of 5 m; (C) On the west beach taken from the ground; (D) On the east beach taken from the ground.

**Table 1.** Location, date, time, weather, purpose of the images, and objects photographed in each investigation conducted by UAV survey.

|                      | Narugashima<br>island | Narugashima<br>island | Narugashima<br>island | Kyoto University<br>Experimental Station | Narugashima<br>island |
|----------------------|-----------------------|-----------------------|-----------------------|--|-----------------------|
| location             | East and west beach   | West beach            | West beach            | Kamigamo Experimental<br>Station         | West beach            |
| date                 | November 27           | December 4            | December 4            | December 16                              | January 25            |
| time                 | 12:00–15:00           | 10:00–15:00           | 15:00–16:00           | 14:00–15:00                              | 10:00–15:00           |
| weather              | Sunny                 | Sunny                 | Sunny                 | Sunny                                    | Sunny                 |
| Purpose of<br>images | Training              | Test                  | Training              | Training                                 | Test                  |
| objects              | Marine debris         | Marine debris         | PET bottle            | PET bottle                               | Marine debris         |

### Data augmentation

Deep learning requires a large amount of training data to avoid overfitting. Therefore, we augmented the training datasets using the ‘imgaug’ python library. For each image, image scaling, random erasing, and contrast changes were applied with a probability of 50%. For random erasing, a rectangular region of 10% of the image size was created and filled with random RGB values in order to detect partially hidden objects during identification. To mask the part of the image, 5–10 of these rectangular areas were randomly generated. Finally, contrast changes were randomly varied between 50% and 200% to correspond to sunlight exposure.

### RetinaNet

In this study, we trained the model using RetinaNet (Lin *et al* 2017), an object detection model derived from region-based convolutional neural networks (Girshick *et al* 2016). RetinaNet consists of a backbone network and two subnetworks. The depth was set to 50 because the F-score is the highest in parameter tuning (supplementary information 1 (available online at [stacks.iop.org/ERC/4/015003/mmedia](https://stacks.iop.org/ERC/4/015003/mmedia))). We set the depth to 50, the epochs to 60, and the batch size to 6 for training. A threshold of more than 0.5 for the score was used for our model to detect marine debris. In addition, non-maximum suppression (NMS) was applied after object detection (Girshick *et al* 2014). NMS is a method that integrates multiple detections of the same object into a single result. In this experiment, the object with the highest probability was used as the standard, and other objects with more than 50% overlap with the standard were removed.

### Orthomosaic images

The same marine debris may have been identified multiple times because overlapping images were taken. Therefore, orthorectified images were used for identification using the Agisoft PhotoScan software. This software uses the Structure from Motion algorithm to create orthomosaic images from overlapping images. In this study, we used 200 images to create each orthomosaic image from a total of 4,421 images. Some areas were not orthorectified and were displayed in white due to low image overlap. Therefore, we processed the data to avoid detection when areas had more than 80% white pixels.

### Accuracy assessment

We segmented the orthorectified images created for the test set with the same size as training images. After identification, an observer randomly selected 100 images to calculate the true positive (TP), false negative (FN), and false positive (FP) rates. We defined FNs when marine debris larger than 100 pixels was not identified. The model was evaluated using sensitivity, precision, and the F-score. For these indices, the following equations were used: sensitivity =  $TP / (TP + FN)$ ; precision =  $TP / (TP + FP)$ ; and F-score =  $2TP / (2TP + FP + FN)$ . Changes in the marine debris were quantified by comparing the number of pieces and the area. The comparison sites were selected from the north, central, and south parts of each beach. Our model marks the detected marine debris with a blue frame. The number of blue frames surrounding the marine debris was defined as counts of marine debris, and we compared the number of marine debris per orthorectified image for each comparison site. The area of the marine debris was calculated using the following method: First, the area containing the blue frame was calculated. Next, the area of the marine debris within the blue frame was calculated for 100 randomly selected samples, which was used as the average marine debris percentage. Finally, the total area of the blue-framed areas in the comparison site was calculated and multiplied by the average marine debris percentage to obtain the estimated area of marine debris. The actual length per pixel in the images was calculated by measuring the size of the PET bottle. ImageJ was used to calculate the area of the blue boxes and marine debris.

## Results

The deep learning model successfully identified marine debris in the high-resolution images (figure 3). For data from Narugashima Island in December 4, the sensitivity was 59% and the precision was 90% (table 2). On the other hand, for the data taken in January 25, the sensitivity was 43% and the precision was 62%. The average of both results was 51% for sensitivity and 76% for precision. The main FPs were waves and rocks (figure 4), and when the marine debris contacted driftwood, it was not detected (figure 5).

As a result of the identification by our deep learning model, the numbers of marine debris at the site on December 4 were 53, 297, and 118 pieces in the north, central, and south parts of the beach, respectively (table 3). The mean number of marine debris ( $\pm$ standard error (SE)) was 156 pieces ( $\pm$ 72.95 pieces). On January 25, the numbers of marine debris at the comparison site were 80, 30, and 93 pieces in the north, central, and south parts of the beach, respectively. The mean number of marine debris ( $\pm$ SE) was 68 pieces ( $\pm$ 19.20 pieces). On December 4, the marine debris density was 0.12, 0.66, and 0.26 pieces/m<sup>2</sup> in the north, center, and south, respectively. The average marine debris density ( $\pm$  SE) was 0.35 pieces/m<sup>2</sup> ( $\pm$ 0.16 pieces/m<sup>2</sup>), and the marine debris density on January 25 was 0.18, 0.06, and 0.21 pieces/m<sup>2</sup> in the north, center, and south, respectively. On this observation date, the average marine debris density on this observation date ( $\pm$ SE) was 0.15 pieces/m<sup>2</sup> ( $\pm$ 0.04 pieces/m<sup>2</sup>).

The areas of marine debris decreased more on January 25 than on December 4. By calculating the actual length of the pixels, the area of the debris could be calculated from the images. The actual length of one pixel ( $\pm$ SE) was 1.06 mm ( $\pm$ 0.04 mm). Based on this length, the areas of the blue frames on December 4 were 2.77, 12.81, and 3.94 m<sup>2</sup> in the north, central, and south part of the beach, respectively. The average blue-framed area ( $\pm$  SE) was 6.51 m<sup>2</sup> ( $\pm$ 3.17 m<sup>2</sup>). On January 25, the areas of the blue frames were 3.95, 4.26, and 6.12 m<sup>2</sup> in the north, central, and south beach, respectively. The average blue-framed area ( $\pm$  SE) was 4.78 m<sup>2</sup> ( $\pm$ 0.68 m<sup>2</sup>). The mean marine debris percentage in the blue-framed area ( $\pm$  SE) was 62.6% ( $\pm$ 1.77%). Based on this percentage, the areas of marine debris on December 4 were 1.74, 8.02, and 2.47 m<sup>2</sup> in the north, center, and south, respectively. The average area ( $\pm$ SE) was 4.08 m<sup>2</sup> ( $\pm$ 1.99 m<sup>2</sup>). The areas of marine debris on January 25 were 2.48, 2.67, and 3.83 m<sup>2</sup> in the north, center, and south, respectively. The average area ( $\pm$  SE) was 2.99 m<sup>2</sup> ( $\pm$ 0.42 m<sup>2</sup>).

The area coverages could also be estimated from the images. The area coverages of marine debris were 0.41%, 1.79%, and 0.54% in the north, central, and south parts of the beach in December 4. The average area ( $\pm$  SE) was 0.92% ( $\pm$ 21.16%). Similarly, the area of marine debris was 0.57%, 0.56%, and 0.86% at the three parts of the beach, respectively, in January 25. The average area ( $\pm$  SE) was 0.66% ( $\pm$ 3.88%). The number and area coverages of marine debris were lower in January compared to December. In addition, it was demonstrated that deep learning could identify marine debris from UAV images and that changes in the debris could be quantified.

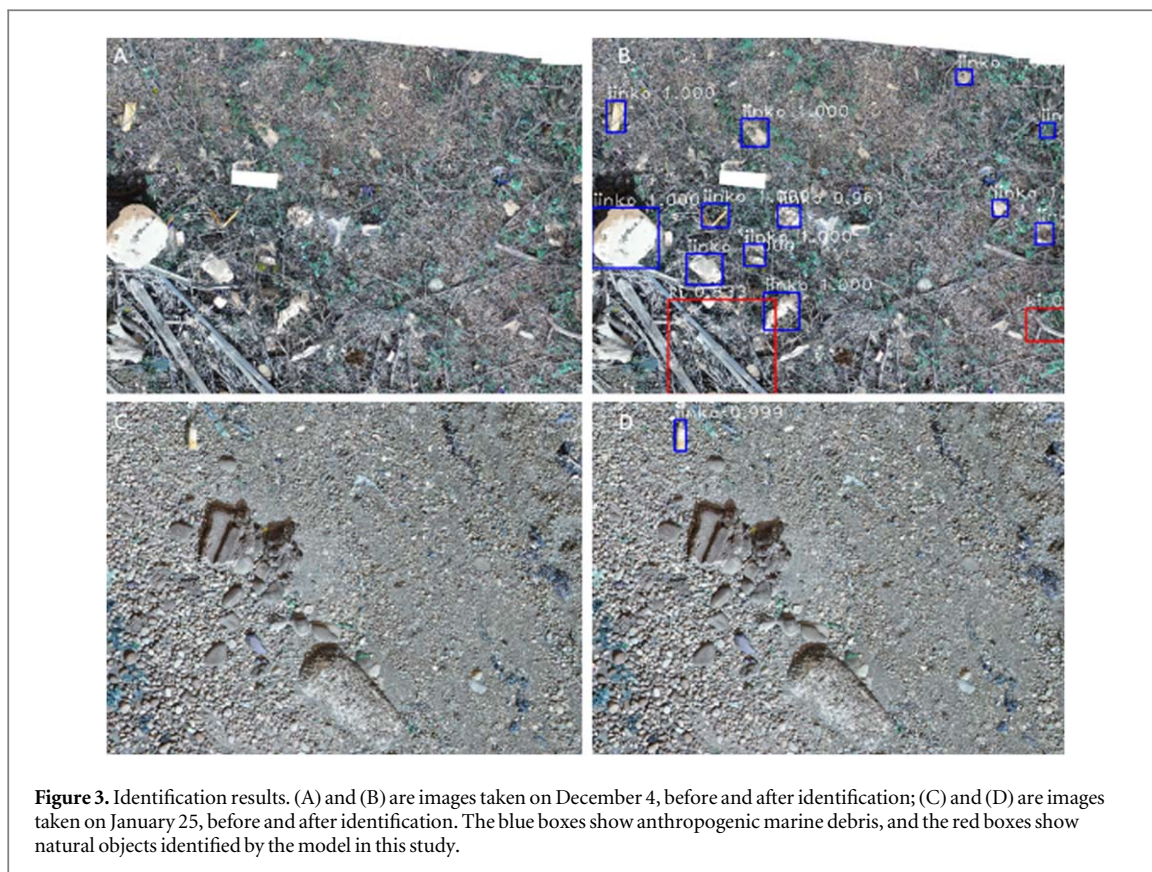


**Table 2.** Identification results and comparison with previous studies.

| Algorithm                           | Area                     | TP    | FN    | FP   | Sensitivity | Precision | F-score |
|-------------------------------------|--------------------------|-------|-------|------|-------------|-----------|---------|
| Martin <i>et al</i> 2018            | Saudi Arabia             | 164   | 251   | 1941 | 0.40        | 0.08      | 0.13    |
| Fallati <i>et al</i> 2019 (Average) | Maldives                 | 57.9  | 74    | 48.9 | 0.44        | 0.54      | 0.49    |
| Our algorithm                       | Narugashima (December 4) | 283   | 200   | 30   | 0.59        | 0.90      | 0.71    |
|                                     | Narugashima (January 25) | 78    | 103   | 48   | 0.43        | 0.62      | 0.51    |
|                                     | Narugashima (Average)    | 180.5 | 151.5 | 30   | 0.51        | 0.76      | 0.61    |

## Discussion

In this study, high-resolution images of marine debris were acquired by combining a UAV equipped with a zoom lens and low altitude flight operation. In addition, the study showed that UAV images can be used for the object detection of marine debris. Although UAVs have also been used in marine debris surveys, high-resolution image acquisition was a challenge. For example, the resolution in the previous study was 4.4 mm/pixel when the DJI Phantom 4 was used at 10 m and 5.0 mm/pixel when it was used at 17 m (Fallati *et al* 2019; Kako *et al* 2020). In this study, a resolution of 1.1 mm/pixel was obtained using the DJI Mavic 2 zoom from an altitude of 5 m. The resolution of the present study was high compared to previous studies, and it was achieved using the combined approach of a UAV that was equipped with the zoom lens and operated from a low altitude.

The advantage of UAVs is that the vehicles can perform survey at a low cost, so periodic monitoring can reveal the spatio-temporal distribution of marine debris. In this study, we acquired 4,421 images and performed an intensive survey at a low altitude to obtain high-resolution images from the target area. Our survey over an area of 0.81-ha was implemented by replacing the battery 12 times. To the best of our knowledge, this is the first study in which a UAV equipped with a zoom camera was operated at a 5 m altitude to identify marine debris.

Our model achieves a sensitivity of 0.59 because of the high-resolution images from the UAV. Moreover, our model could identify anthropogenic marine debris from the wide variety of objects on a beach. Training data containing multiple types of debris enabled the high performance of our model. In addition, we annotated two classes, anthropogenic marine debris and natural objects, allowing the model to distinguish between human and natural-origin debris. The types and composition of these categories differ, and annotating typical natural objects improved the performance of the model.



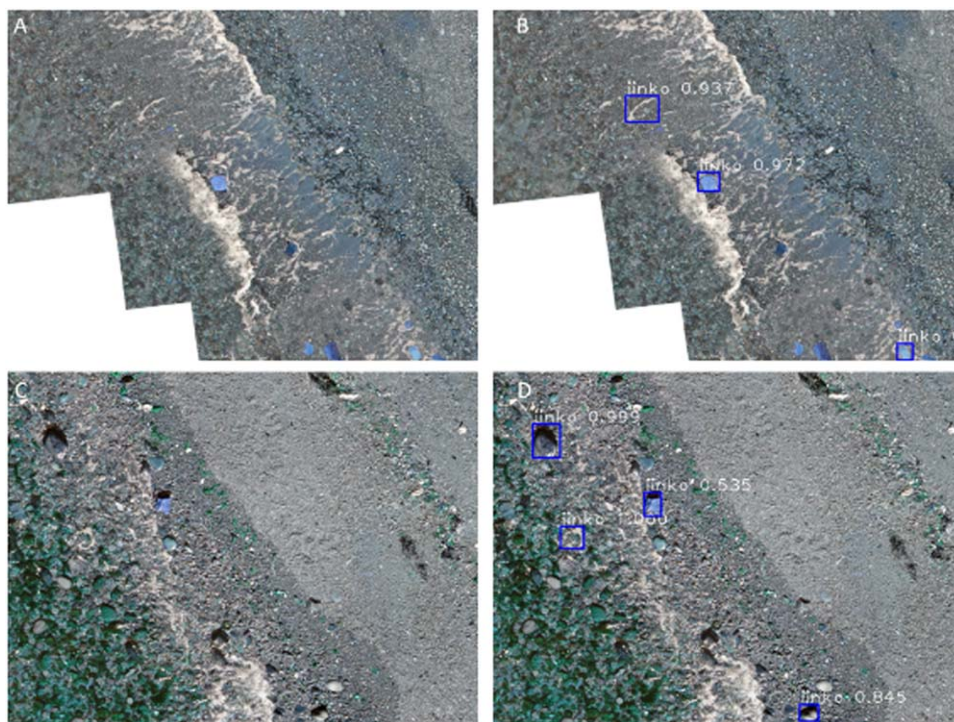


**Figure 4.** Major false positive images. (A) and (B) are before and after images, respectively, taken in December 4; (C) and (D) are before and after images, respectively, taken in January 25.

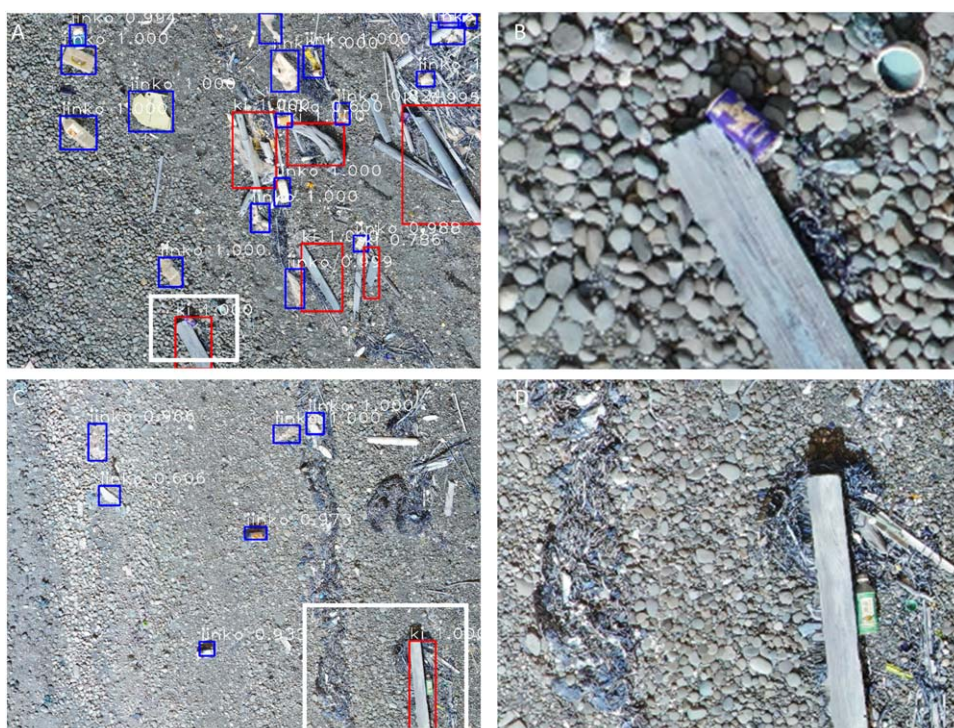


**Figure 5.** Unidentified marine debris owing to partial interference of driftwood. The images of (A) and (B) are taken on December 4; (C) and (D) are taken on January 25. (B) and (D) are partial expanded view of the white frames of (A) and (C), respectively. The wood in this image has been artificially processed. This study targeted marine debris made of anthropogenic material such as plastic, glass, and metal; wood was excluded because it decomposes naturally.

Our technique evinced a decrease in marine debris through cleanup activities. These activities have been performed worldwide on beaches. However, continuously monitoring a large area after cleanup activities is labor-intensive. In our study, we found that combining UAVs and deep learning makes it possible to compare

**Table 3.** Comparison of the number of marine debris and the area observed. Average and standard error (SE) are also given for each set.

| Date       | Comparison sites | Number of debris (blue frame) | Number of debris per comparison sites (pieces m <sup>2</sup> ) | Area of debris per comparison sites (%) |
|------------|------------------|-------------------------------|--|---|
| December 4 | North            | 53                            | 0.12   | 0.41                                    |
|            | Central          | 297                           | 0.66   | 1.79                                    |
|            | South            | 118                           | 0.26   | 0.54                                    |
|            | <b>Average</b>   | <b>156.00</b>                 | <b>0.35</b>  | <b>0.92</b>                             |
|            | <b>SE</b>        | <b>72.95</b>                  | <b>0.16</b>  | <b>21.16</b>                            |
| January 25 | North            | 80                            | 0.18   | 0.57                                    |
|            | Central          | 30                            | 0.06   | 0.56                                    |
|            | South            | 93                            | 0.21   | 0.86                                    |
|            | <b>Average</b>   | <b>67.67</b>                  | <b>0.15</b>  | <b>0.66</b>                             |
|            | <b>SE</b>        | <b>19.20</b>                  | <b>0.04</b>  | <b>3.88</b>                             |

the amount of debris before and after a cleanup activity and quantify the effectiveness of the cleanup effort. Moreover, we clarified that the distribution of marine debris varied depending on the site. Ocean currents and wind direction may affect marine debris distribution. In the future, continuous surveys using this technique might reveal the factors behind marine debris accumulation.

Despite using the same model, the identification accuracy differed, as sensitivity decreased when the test images were taken on January 25. The reduction in the amount of marine debris on the beach may affect the model's sensitivity, and more marine debris could be detected by changing the threshold of our model. In addition, detecting entangled debris in vegetation was challenging. Furthermore, the orientation of the marine debris may affect the results. Debris entangled in vegetation can be scattered at various angles, and the training images did not contain these varied angles. Therefore, improving the training images will improve the model performance.

Our model underestimated the amount of marine debris owing to a high false negatives. Previous studies have shown that identifying marine debris using UAVs also underestimates the amount of debris compared to a human ground survey (Martin *et al* 2018). The shadows of debris can also affect identification, and it is recommended that UAVs be operated around noon to reduce shadows (Martin *et al* 2018; Lo *et al* 2020). In our study, the images were consecutively taken between 10:00 and 15:00. Therefore, the high false negatives may be attributed to the Sunlight conditions in each image.

Some limitations still exist in this study. First, detecting small anthropogenic marine debris such as fragments of plastic products is difficult. The criteria for the annotation also affect the low detection of small debris. Marine debris was annotated if the size was larger than 100 pixels because it was difficult to annotate all of the debris. Further consideration of criteria for the annotation will be needed to detect the smaller size of debris. Second, the results of our study show lower sensitivity, indicating that the model cannot detect all marine debris because of the excesses of false negatives. A variety of anthropogenic marine debris was annotated as one class, such as PET bottles, plastic bags, and cans. Therefore, separating the class into more subdivided categories may improve the sensitivity. Although high-resolution images acquired operated UAV at a low altitude, this operation required multiple batteries; for example, batteries were replaced 12 times in this study. In addition, operations over several hours also affect the light conditions of the image; thus, this difference may have affected the performance. Additionally, object detection was used in this study, but it may be necessary to consider other approaches, such as semantic segmentation for more accurate estimation. Finally, our results show microplastic detection is quite challenging; however, monitoring these distributions is essential to understanding plastic pollution in the marine environment. Citizen science can also be beneficial to survey microplastic pollution with other protocols.

Although beaches attract attention as places that often accumulate marine debris, few studies have identified marine debris on beaches using UAVs combined with deep learning (Fallati *et al* 2019). Some studies used aircraft to survey the distribution of marine debris (Moy *et al* 2018); however, the cost is prohibitive. The advantage of UAVs is that they can acquire higher-resolution images at a lower cost than aircraft. In addition, UAVs enable safe surveys in dangerous areas where marine debris accumulates, such as areas containing medical waste. In these areas, remote sensing surveys of beaches using UAVs can be conducted. Using UAVs is also beneficial from an ecological perspective (Harris *et al* 2015). Beaches are essential for the breeding of some species of marine wildlife. For example, the human use of beaches affects areas where sea turtles lay their eggs (Antworth *et al* 2006) and the behavior of seabirds (Burger and Niles, 2013). Thus, minimizing disturbance to marine wildlife by conducting surveys without directly entering the beach is possible.

The present study, showed that deep learning could identify marine debris obtained from high-resolution UAVs images. Marine debris is expected to increase in the future, and the monitoring is an urgent global issue.

Using UAVs and deep learning will allow for uniform surveys to be conducted worldwide at a low cost. To help solve the marine debris problem, it is necessary to clarify the current situation at a global scale. Citizen science in obtaining marine debris has continued to grow (Sandahl and Tøttrup 2020), and our model can be used to evaluate cleanup activities. The worldwide use of methods such as those described in this study, which combines field surveys and information science technology, will help enable the efficient management of marine debris.

## Acknowledgments

We thank Y Sasaki, H Iejima, N Itou for their assistance and for providing valuable comments to our research. Furthermore, we appreciate the staff of the Kamigamo Experimental Station, Field Science Education and Research Center, Kyoto University, for supporting our field survey. This study was supported by the Re:connect Program of the Nippon Foundation-Kyoto University Joint Project.

## Data availability statement

All data that support the findings of this study are included within the article (and any supplementary files).

## Conflict of interest statement

The authors declare no conflicts of interest associated with this manuscript.

## Author contribution statement

KT performed the field surveys and experiments and wrote the manuscript. AS performed the field surveys and experiments. YM created the deep learning model. TI guided all steps of the experiments and manuscript preparation.

## ORCID iDs

Kosuke Takaya  <https://orcid.org/0000-0003-1415-6287>

## References

- Andrady A L 2011 Microplastics in the marine environment *Mar. Pollut. Bull.* **62** 1596–605
- Andriolo U, Gonçalves G, Bessa F and Sobral P 2020 Mapping marine litter on coastal dunes with unmanned aerial systems: a showcase on the atlantic coast *Sci. Total Environ.* **736** 139632
- Antworth R L, Pike D A and Stiner J C 2006 Nesting ecology, current status, and conservation of sea turtles on an uninhabited beach in Florida, USA *Biological Conservation* **130** 10–5
- Bao Z, Sha J, Li X, Hanchiso T and Shifaw E 2018 Monitoring of beach litter by automatic interpretation of unmanned aerial vehicle images using the segmentation threshold method *Mar. Pollut. Bull.* **137** 388–98
- Barnes D K, Galgani F, Thompson R C and Barlaz M 2009 Accumulation and fragmentation of plastic debris in global environments *Philos. Trans. R. Soc. London, Ser. B* **364** 1985–98
- Brennan E, Wilcox C and Hardesty B D 2018 Connecting flux, deposition and resuspension in coastal debris surveys *Sci. Total Environ.* **644** 1019–26
- Burger J and Niles L 2013 Shorebirds and stakeholders: effects of beach closure and human activities on shorebirds at a New Jersey coastal beach *Urban Ecosystems* **16** 657–73
- Chiba S, Saito H, Fletcher R, Yogi T, Kayo M, Miyagi S, Ogido M and Fujikura K 2018 Human footprint in the abyss: 30 year records of deep-sea plastic debris *Marine Policy* **96** 204–12
- Cho D O 2011 Removing derelict fishing gear from the deep seabed of the east sea *Marine Policy* **35** 610–4
- Cole M, Lindeque P, Halsband C and Galloway T S 2011 Microplastics as contaminants in the marine environment: a review *Mar. Pollut. Bull.* **62** 2588–97
- Cózar A *et al* 2014 Plastic debris in the open ocean *Proc. Natl. Acad. Sci. U.S.A.* **111** 10239–44
- Dai Z, Zhang H, Zhou Q, Tian Y, Chen T, Tu C, Fu C and Luo Y 2018 Occurrence of microplastics in the water column and sediment in an inland sea affected by intensive anthropogenic activities *Environ. Pollut.* **242** 1557–65
- Deidun A, Gauci A, Lagorio S and Galgani F 2018 Optimising beached litter monitoring protocols through aerial imagery *Mar. Pollut. Bull.* **131** 212–7
- Derraik J G 2002 The pollution of the marine environment by plastic debris: a review *Mar. Pollut. Bull.* **44** 842–52
- Eriksen M, Lebreton L C, Carson H S, Thiel M, Moore C J, Borroero J C, Galgani F, Ryan P G and Reisser J 2014 Plastic pollution in the world's oceans: more than 5 trillion plastic pieces weighing over 250,000 tons afloat at sea *PLoS One* **9** e111913
- Fallati L, Polidori A, Salvatore C, Saponari L, Savini A and Galli P 2019 Anthropogenic marine debris assessment with unmanned aerial vehicle imagery and deep learning: a case study along the beaches of the republic of maldives *Sci. Total Environ.* **693** 133581

- Fujieda Shigeru, Hoshika A, Hashimoto E, Sasakura Satoshi, Shimizu Takanori and Okumura Masataka 2010 Budget of marine litter in the seto inland sea *Journal of Coastal Zone Studies* **22** 17–29 <http://seafrogs.info/marinelitter/enganik224.pdf>
- Gall S C and Thompson R C 2015 The impact of debris on marine life *Mar. Pollut. Bull.* **92** 170–9
- Girshick R, Donahue J, Darrell T and Malik J 2014 Rich feature hierarchies for accurate object detection and semantic segmentation *Proc. of the IEEE Conference On Computer Vision And Pattern Recognition* 580–587 ([https://openaccess.thecvf.com/content\\_cvpr\\_2014/papers/Girshick\\_Rich\\_Feature\\_Hierarchies\\_2014\\_CVPR\\_paper.pdf](https://openaccess.thecvf.com/content_cvpr_2014/papers/Girshick_Rich_Feature_Hierarchies_2014_CVPR_paper.pdf))
- Girshick R, Donahue J, Darrell T and Malik J 2016 Region-based convolutional networks for accurate object detection and segmentation *IEEE Trans. Pattern Anal. Mach. Intell.* **38** 142–58
- Gonçalves G, Andriolo U, Pinto L and Bessa F 2020 Mapping marine litter using UAS on a beach-dune system: a multidisciplinary approach *Sci. Total Environ.* **706** 135742
- Gregory M R 2009 Environmental implications of plastic debris in marine settings—entanglement, ingestion, smothering, hangers-on, hitch-hiking and alien invasions *Philos. Trans. R. Soc. London, Ser. B* **364** 2013–25
- Harris L, Nel R, Holness S and Schoeman D 2015 Quantifying cumulative threats to sandy beach ecosystems: a tool to guide ecosystem-based management beyond coastal reserves *Ocean & Coastal Management* **110** 12–24
- Iñiguez M E, Conesa J A and Fullana A 2016 Marine debris occurrence and treatment: a review *Renew. Sustain. Energy Rev.* **64** 394–402
- Jambeck J R, Geyer R, Wilcox C, Siegler T R, Perryman M, Andrady A, Narayan R and Law K L 2015 Marine pollution *Plastic Waste Inputs from Land Into The Ocean. Science* **347** 768–71
- Jiménez López J and Mulero-Pázmány M 2019 *UAVs for Conservation In Protected Areas: Present and Future. UAVS.* **3** 10
- Kako S I, Isobe A and Magome S 2012 Low altitude remote-sensing method to monitor marine and beach litter of various colors using a balloon equipped with a digital camera *Mar. Pollut. Bull.* **64** 1156–62
- Kako S I, Morita S and Taneda T 2020 Estimation of plastic marine debris volumes on beaches using unmanned aerial vehicles and image processing based on deep learning *Mar. Pollut. Bull.* **155** 111127
- Lavers J L and Bond A L 2017 Exceptional and rapid accumulation of anthropogenic debris on one of the world's most remote and pristine islands *Proc. Natl. Acad. Sci. U.S.A.* **114** 6052–5
- Law K L and Thompson R C 2014 Oceans *Microplastics in The Seas. SCIENCE* **345** 144–5
- Lin T Y, Goyal P, Girshick R, He K and Dollár P 2017 Focal loss for dense object detection *Proc. of The IEEE International Conference On Computer Vision(2980–2988)* ([https://openaccess.thecvf.com/content\\_ICCV\\_2017/papers/Lin\\_Focal\\_Loss\\_for\\_ICCV\\_2017\\_paper.pdf](https://openaccess.thecvf.com/content_ICCV_2017/papers/Lin_Focal_Loss_for_ICCV_2017_paper.pdf))
- Lo H S, Wong L C, Kwok S H, Lee Y K, Po B H K, Wong C Y, Tam N F and Cheung S G 2020 Field test of beach litter assessment by commercial aerial UAV *Mar. Pollut. Bull.* **151** 110823
- Martin C, Parkes S, Zhang Q, Zhang X, McCabe M F and Duarte C M 2018 Use of unmanned aerial vehicles for efficient beach litter monitoring *Mar. Pollut. Bull.* **131** 662–73
- Martin C, Zhang Q, Zhai D, Zhang X and Duarte C M 2021 Enabling a large-scale assessment of litter along Saudi Arabian red sea shores by combining UAVs and machine learning *Environ. Pollut.* **277** 116730
- McIlgorm A, Campbell H F and Rule M J 2011 The economic cost and control of marine debris damage in the Asia-Pacific region *Ocean & Coastal Management* **54** 643–51
- Merlino S, Paterni M, Berton A and Massetti L 2020 Unmanned aerial vehicles for debris survey in coastal areas: long-term monitoring programme to study spatial and temporal accumulation of the dynamics of beached marine litter *Remote Sensing* **12** 1260
- Moy K, Neilson B, Chung A, Meadows A, Castrence M, Ambagis S and Davidson K 2018 Mapping coastal marine debris using aerial imagery and spatial analysis *Mar. Pollut. Bull.* **132** 52–9
- Olivelli A, Hardesty B D and Wilcox C 2020 Coastal margins and backshores represent a major sink for marine debris: insights from a continental-scale analysis *Environ. Res. Lett.* **15** 074037
- Ostle C, Thompson R C, Broughton D, Gregory L, Wootton M and Johns D G 2019 The rise in ocean plastics evidenced from a 60-year time series *Nat. Commun.* **10** 1–6
- Papakonstantinou A, Batsaris M, Spondylidis S and Topouzelis K 2021 A citizen science unmanned aerial system data acquisition protocol and deep learning techniques for the automatic detection and mapping of marine litter concentrations in the coastal zone *UAVS* **5** 6
- Sandahl A and Tøttrup A P 2020 Marine citizen science: recent developments and future recommendations *Citizen Science: Theory and Practice* **5** 24
- Sathish N, Jayasanta K I and Patterson J 2019 Abundance, characteristics and surface degradation features of microplastics in beach sediments of five coastal areas in Tamil Nadu, India *Mar. Pollut. Bull.* **142** 112–8
- Singh B and Sharma N 2008 Mechanistic implications of plastic degradation *Polym. Degrad. Stab.* **93** 561–84
- Topouzelis K, Papakonstantinou A and Garaba S P 2019 Detection of floating plastics from satellite and unmanned aerial systems (plastic litter project 2018) *Int. J. Appl. Earth Obs. Geoinf.* **79** 175–83
- Willis K, D Hardesty B D, Kriwoken L and Wilcox C 2017 Differentiating littering, urban runoff and marine transport as sources of marine debris in coastal and estuarine environments *Sci. Rep.* **7** 44479
- Woodall L C, Sanchez-Vidal A, Canals M, Paterson G L, Coppock R, Sleight V, Calafat A, Rogers A D, Narayanaswamy B E and Thompson R C 2014 The deep sea is a major sink for microplastic debris *Royal Society Open Science* **1** 140317
- Yamashita R and Tanimura A 2007 Floating plastic in the kuroshio current area, western north pacific ocean *Mar. Pollut. Bull.* **54** 485–8